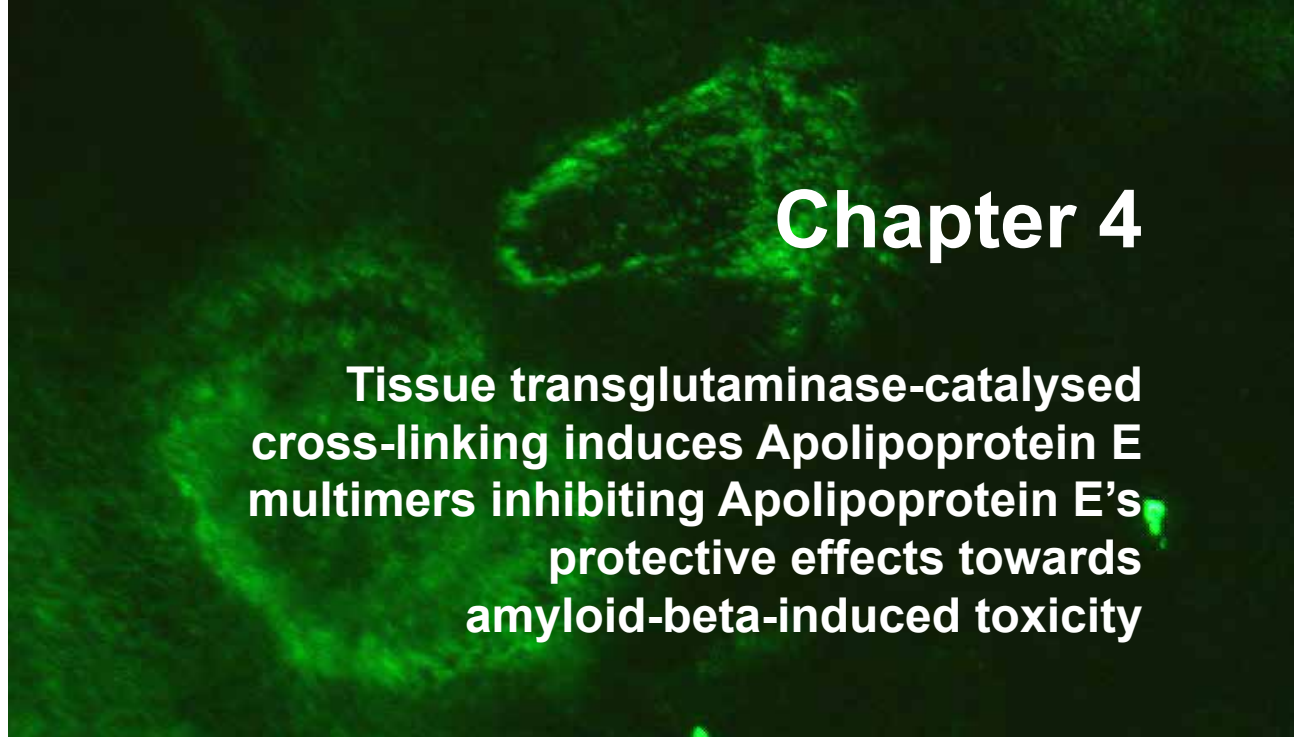

Chapter 4

Tissue transglutaminase-catalysed cross-linking induces Apolipoprotein E multimers inhibiting Apolipoprotein E's protective effects towards amyloid-beta-induced toxicity

Mieke de Jager
Benjamin Drukarch
Marloes Hofstee
John Brevé
Cornelis A.M. Jongenelen
John G.J.M. Bol
Micha M.M. Wilhelmus

Department of Anatomy and Neurosciences, Neuroscience Campus Amsterdam, VU University Medical Center, Amsterdam, The Netherlands

Journal of Neurochemistry 2015; 134(6):1116-28

Abstract

Cerebral amyloid angiopathy (CAA) is a pathological hallmark of Alzheimer's disease (AD) and characterised by deposition of amyloid-β (Aβ) protein and smooth muscle cell (SMC) death in cerebral vessel walls. Apolipoprotein E (ApoE) is of importance in both Aβ accumulation and Aβ-mediated toxicity towards SMCs in the cerebral vessel wall, although its exact role in CAA pathogenesis remains unclear. Tissue transglutaminase (tTG) is an enzyme capable of inducing both protein complexes and altered protein bioactivity via post-translational cross-linking. In CAA, tTG and its catalytic activity are associated with deposited Aβ. Furthermore, several apolipoproteins are known substrates of tTG. We therefore investigated whether ApoE is a substrate for tTG and if this affects ApoE's bioactivity. We found strong binding of different ApoE isoforms with tTG and demonstrated tTG-catalysed ApoE multimers. In post-mortem human AD cases, ApoE colocalised with in situ active tTG in CAA. Moreover, human brain SMCs treated with Aβ demonstrated enhanced secretion of both ApoE and tTG, and of TG cross-links in the extracellular matrix. Interestingly, tTG-catalysed cross-linked ApoE failed to protect SMCs against Aβ-mediated cytotoxicity. Together, our data demonstrate a novel tTG-driven post-translational modification of ApoE that might play an important role in CAA.

Introduction

Alzheimer's disease (AD) is characterised by the deposition of amyloid-beta (Aβ) in parenchymal senile plaques (SPs) as well as in the cerebral vessel walls as cerebral amyloid angiopathy (CAA) [1]. CAA is present in over 90% of AD patients, contributes to the rate of cognitive decline in AD patients, and is characterised by Aβ-mediated degeneration of smooth muscle cells (SMCs), ultimately leading to brain haemorrhages [2, 3]. Apolipoprotein E (ApoE) has been identified as a major risk factor for the sporadic late-onset form of AD. The ApoE gene has three alleles, ε2, ε3 and ε4, the most frequent of which is the ε3 allele. Inheritance of one or two copies of the ε4 allele is associated with a dose-dependent increased risk for AD, a higher load of CAA, and an earlier age of onset of AD [4–7]. Moreover, ApoE protein is present in CAA in AD cases [8, 9] and in vitro studies have shown that ApoE is able to bind, transport and clear Aβ from the brain [10, 11] depending on both isoform (ε2>ε3>ε4) and lipidation state [12]. Interestingly, ApoE plays an important role in the protection of cerebral SMCs against Aβ-induced cytotoxicity [13]. However, mechanisms underlying the apparent failure of this protective role against Aβ-induced cytotoxicity of cerebral SMCs in CAA remain unclear.

The transglutaminase (TG) protein family (EC 2.3.2.13) consists of nine members, including tissue transglutaminase (tTG). tTG plays an important role during development, cell differentiation and apoptosis [14]. TGs are calcium-dependent enzymes that catalyse several reactions, in particular the formation of molecular cross-links [15]. TGs induce such cross-links by catalysing an acyl transfer reaction between the γ-carboxamide group of a polypeptide-bound glutamine and the ε-amino group of a polypeptide bound lysine residue to form a covalent ε-(γ-glutamyl)lysine isopeptide bond, either within or between proteins [16]. This cross-linking activity therefore is capable of stably altering the conformation of proteins and/or induces formation of protein multimers and complexes [17, 18]. As a result of this post-translational modification, bioactivity of proteins is strongly altered, e.g. conversion of monomer interleukin-2 into a highly toxic dimer [19].

Evidence is mounting that tTG and its transamidation activity play an important role in AD pathogenesis [20–22]. In AD brains, tTG levels and its cross-links are elevated [23–25] and correlate with the cognitive decline observed in these patients [25, 26]. Furthermore, Aβ is a substrate for tTG-mediated cross-linking [18, 27–30], and we recently demonstrated that tTG and its activity are associated with both early and end-stage CAA [20, 21].

Apolipoproteins are known to be post-translationally modified via glycosylation [31], proteolytic processing [32, 33] and fatty acylation [34]. Interestingly, apolipoprotein family members A-I, A-II, B and C-I are substrates for TG-catalysed cross-linking [35, 36], resulting in their polymerisation. Although the functional significance of the TG-catalysed cross-linking of apolipoproteins is still unclear, these cross-links are suggested to play an

important role in both their structure and complex formation with other proteins and lipids [35, 36].

To investigate whether tTG-mediated post-translational cross-linking of ApoE may play a role in Aβ-induced cerebral SMC degeneration in CAA, in the current study, we first analysed whether ApoE is a substrate for TG-catalysed cross-linking and if this cross-linking of ApoE results in ApoE multimerisation. Moreover, we studied colocalisation of in situ active tTG with ApoE in CAA in post-mortem brain tissue of AD cases. Treatment of cerebrovascular cells with Aβ induces upregulation and secretion of ApoE, and this extracellular ApoE protects cerebrovascular cells from Aβ-induced cell death [13]. As a follow up of this study, we here investigated if Aβ treatment of human brain vascular smooth muscle cells (HBV-SMCs), in addition to ApoE, induces secretion of catalytically active tTG into the extracellular matrix and whether tTG-mediated cross-linking of ApoE affects its protective role towards Aβ-induced cell death of HBV-SMC.

Materials and Methods

Preparation of peptides

Human recombinant ApoE2, 3, and 4 produced in S. frugiperda were obtained from Merck Millipore (Billerica, MA, USA) and human plasma purified ApoE3 (ApoE3L) from rPeptide (A-2001-1, Bogart, GA, USA). Human recombinant tTG (T002, Zedira GmbH, Darmstadt, Germany) was reconstituted in MilliQ water at a stock concentration of 1mg/ml. Human $A\beta_{1-42}$ (rPeptide, Bogart, GA, USA) and human $A\beta_{1-40}$ (Innovagen, Lund, Sweden) were dissolved in sterile MilliQ water at a concentration of 250μM. For Thioflavin T assay human $A\beta_{1-42}$ (rPeptide) was dissolved directly in hexafluoro-2-propanol (Sigma-Aldrich, St. Louis, Missouri, USA) and subsequently air-dried overnight and then dissolved in dimethylsulfoxide (DMSO) at a final concentration of 5mM. Aliquots of all peptide preparations were stored at -80°C.

Surface plasmon resonance (SPR)

SPR experiments were performed using a BIAcore 2000 biosensor instrument (Biacore, Uppsala, Sweden), as described previously [37]. Sensor chips and protein coupling chemicals were purchased from Biacore. Human recombinant ApoE2, 3, 4 produced in S. frugiperda and human plasma purified ApoE3 (ApoE3L) (25 μM dissolved in 10 mM Na-acetate, pH 3.5) were coupled to the surface of the sensor flow cell. Kinetic measurements were performed at 25°C with a flow rate of 10 μl/min in 10 mM 4-(2-hydroxyethyl)-1-piperazineethanesulfonic acid (HEPES), pH 7.4, 150 mM NaCl, 3 mM ethylenediaminetetraacetic acid (EDTA), 0.005% (v/v) surfactant P20. Interaction of tTG with ApoE was monitored using 6 different concentrations of human recombinant tTG (0.32-2.6 μM). The sensor surface was regenerated with 20 μl of 10 mM NaOH inducing dissociation of tTG from

ApoE. The BIAcore kinetic evaluation software was used to generate overlay plots of 6 concentrations of tTG to determine the relative dissociation constant KD (expressed in M). All experiments were performed in duplicate per chip, and at least two different sensor chips were used to exclude chip-to-chip variations.

Effects of tTG on ApoE multimerisation

Human recombinant tTG (5 μM) was incubated with 5.3 μM human plasma isolated ApoE (ApoE3L) in a 50 mM Tris-HCl pH 8.0 buffer with 10mM CaCl2 and 5mM dithiothreitol (DTT) for an hour at room temperature (RT). To test for tTG-cross-link activity, ApoE (2.6 μM) and tTG (2.5 μM) were co-incubated with 1 mM of the TG substrate biotinylated 5-(biotinamido)-pentylamine (BAP; Thermo Fisher Scientific, Waltham, MA, USA) in the same buffers for an hour at RT. Samples were mixed with either 6x Tris/glycine sample buffer or 4x LDS (Lithium dodecyl sulfate) sample buffer (Invitrogen, Camarillo, CA, USA) and separated on a 10% SDS-PAGE gel or 4-12% Bis-Tris NuPAGE gel with 2-(N-morpholino) ethanesulfonic acid (MES) running buffer (Invitrogen). Samples were transferred to a polyvinylidene fluoride (PVDF) membrane (Merck Millipore), blocked with 5% non-fat skimmed milk (ELK) (Campina, Woerden, Utrecht, The Netherlands) in Tris-buffered saline (TBS) with 0.1% Tween-20 (5%-ELK-TBST) and incubated overnight at 4°C with primary antibody mouse anti-ApoE (1:1000, D6E1, Abcam Inc, Cambridge, UK) and Streptavidin/Avidin-poly horse-radish peroxidase (1:5000, Abcam) in 2.5% ELK-TBST. Blots were subsequently incubated for 1 hour at RT with secondary antibody goat anti-mouse horse-radish peroxidase (1:1000, DAKO Cytomation, Glostrup, Denmark) and the chemiluminescence substrate (SuperSignal® West Dura Extended Duration Substrate Kit, Thermo Fisher Scientific) was used to visualise bands. In between incubation steps, blots were washed with TBS-T and TBS. Membranes were scanned in a Chemidoc XRS scanner (Bio-Rad Laboratories, Hercules, CA, USA) and band densities were analysed with the Quantity One 4.6 software program (Bio-Rad Laboratories). Graphpad Prism 5 statistical software package and SPSS Statistics 20.0 were used to present and statistically analyse data. A t-test was performed to test for statistical differences between the monomers in the ApoE or ApoE/tTG condition and between the multimers in either condition. Data are presented as mean±SEM.

Electron microscopy (EM) and Thioflavin T assay

Both human recombinant tTG (5 μM) and ApoE3L (5 μM) alone, or tTG co-incubated with ApoE, with or without 5 mM EDTA were incubated in 50 mM Tris-HCl buffer pH 8.0 with 2 mM CaCl2 and 5 mM DTT for 6 hours. To study the morphology of ApoE multimers, the resulting samples were diluted in ultra pure water (1:5) and 5 μl aliquots were allowed to attach for 5 minutes on formvar-coated Ni-grids (Electron Microscopy Sciences, Hatfield, PA, USA) at 37°C. Grids were washed with ultra pure water and air-dried. For EM, samples were negatively stained for 20 minutes with 3% filtered uranyl acetate solution and visual-

ised with a Philips CM 100 electron microscope (Philips, Eindhoven, The Netherlands).
For the Thioflavin T assay, protein samples of $A\beta_{1-42}$ (5 μM), ApoE (5 μM), tTG alone (5 μM) and ApoE co-incubated with tTG were incubated for 1, 3 and 6 hours at RT. Samples were diluted in 5 μM Thioflavin T (ThioT, Sigma-Aldrich) solution in 10 mM Tris–HCl, pH 7.4. Aggregation kinetics were monitored with a Fluostar microplate reader (serial number 403-0139, BMG Labtech, Ortenberg, Germany) at excitation 450nm and emission 485nm, and analysed with Fluostar Galaxy software (version 4.30-0, BMG Labtech).

Human post-mortem brain tissue
Neocortex tissue samples from 5 AD patients with CAA (age 91.0 ± 4.6 years; post-mortem delay 5.0 ± 2.0 hours) and 4 controls without neurological disease (age 81.3 ± 6.6 years; post-mortem delay 7.5 ± 1.0 hours) were used (The Netherlands Brain Bank, Amsterdam, The Netherlands). Brain tissue was rapidly dissected following autopsy and immediately frozen in liquid nitrogen. The diagnosis of AD was based on neuropathological and clinical criteria [38]. Table 1 provides an overview of the diagnosis, score for Aβ and NFTs, CAA grading, age, post-mortem interval and gender of the patients used in this study. CAA grading was established by quantification of the number of Aβ-positive vessels in one microscopic field (magnification 25x), as described in a previous report [39]. At least 4 microscopic fields of neocortex were analysed and categorised as follows: 0 (-, no CAA), 0-10 (+, sparse CAA), 10-20 (++, moderate CAA) and >20 (+++, severe CAA) vessels affected by Aβ deposition.

Table 1 Patients characteristics

Number	Diagnosis	Gender	Age	PMI (hr)	Grade (Braak, NFTs)	Grade (Braak, Aβ)	Grade CAA
1	AD/CAA	F	90	4	C3	A3	+++
2	AD/CAA	F	81	3	C3	A3	+++
3	AD/CAA	F	96	4	C3	A3	+++
4	AD/CAA	F	87	8	C3	A3	+++
5	AD/CAA	F	65	6	C3	A3	+
6	Control	F	87	8	C1	nd	++
7	Control	F	73	8	C1	A2	++
8	Control	M	86	6	C1	A2	++
9	Control	M	79	8	C1	A1	-

Abbreviations: AD = Alzheimer's disease, CAA = cerebral amyloid angiopathy, F = Female, M = Male, PMI = post-mortem interval (h = hours). Grading of NFT, Aβ and CAA severity was performed as described in the materials and methods section. For NFT and Aβ score, classification according to Hyman and colleagues [38] is shown.

Double immunofluorescence
Experiments were performed as described previously [20, 21]. Serial sections of neocortex (6 μm) were fixed with acetone (100%) for 10 minutes and air-dried. Subsequently, sections were blocked with 3% bovine serum albumin (BSA; PAA Laboratories, Pasching, Austria) in TBS with 0.5% TritonX-100 (TBS-T). Primary antibodies mouse anti-ApoE (ApoE ab1906, Abcam) and rabbit anti-Aβ (715800, Invitrogen) were diluted in 3% BSA/TBS-T and incubated overnight at 4°C. Negative controls were incubated in this solution without the primary antibodies. The secondary antibodies donkey anti-mouse or donkey anti-rabbit, both coupled to either Alexa 488 or Alexa 594 (dilution 1:400; Jackson Immunoresearch Laboratories Inc., Suffolk, UK) were diluted in 3% BSA/TBS-T and incubated for 2 hours at RT. In between incubation steps, sections were extensively washed with TBS. Sections were mounted with Vectashield® (Vector laboratories Inc) or PVA-DABCO® mounting medium (Sigma-Aldrich) and visualised using a Leica TCS SP2 AOBS confocal laser scanning microscope (Leica Microsystems, Rijswijk, the Netherlands). To exclude bleed-through of fluorescence emission, a series of images was obtained by sequential scanning of channels through a 40x lens (zoom factor 1 or 2x, resolution 1024x1024).

In situ TG activity
In situ TG activity detection was performed as described previously [21]. In brief, unfixed 6 μm thick tissue sections of neocortex of AD cases were preincubated for 20 minutes at RT in a 100 mM Tris-HCl, pH 7.4, 5mM CaCl2, 1 mM DTT (Promega, Madison, WI, USA) buffer with or without 100 μM of the selective tTG activity inhibitor Z-DON-Val-Pro-Leu-OMe (Z-DON) [40, 41], purchased from Zedira GmbH. Then, incubation was continued for 30 minutes at 37°C with the same incubation buffer with or without inhibitor to which 50μM T26 (Covalab, Villeurbanne, France), a specific tTG substrate [42, 43], was added. Thereafter, sections were washed with MilliQ water, air-dried, fixed for 10 minutes with 100% acetone, blocked with 3%BSA/TBS-T and subsequently incubated with primary antibody mouse anti-ApoE or mouse anti-Aβ (AB10, Merck Millipore) in 3% BSA/TBS-T overnight at 4°C. Secondary antibodies used were donkey anti-mouse coupled to Alexa488 to detect ApoE or Aβ and streptavidin coupled to Alexa594 to detect T26 incorporation (all diluted 1:400, Jackson Immunoresearch Laboratories Inc). Sections were mounted and visualised as described for double immunofluorescence.

Cell culture
Primary human brain vascular smooth muscle cells (HBV-SMCs, Sciencell Research Laboratories, Sanbio, Uden, The Netherlands) were cultured at 37°C under 5% CO2 in air in a 1:1 mixture of Dulbecco's modified Eagle's medium and HAM's F10 nutrient mixture (PAA Laboratories) containing 10% foetal calf serum (FCS), 1% non-essential amino acids (Gibco® Life Technologies, Carlsbad, CA, USA), 2.5 mM L-glutamine and 50 μunits/mL of both penicillin and streptomycin. Cell passages two to seven were used for experiments.

Cells were plated as indicated per experiment and grown until near-confluence. Cells were washed with serum-free medium twice and incubated in serum-free medium for at least four hours. Subsequently, cells were treated with Aβ, ApoE, tTG or MilliQ water (diluent) as indicated per experiment.

Effect of Aβ treatment on ApoE, tTG and TG cross-links in extracellular matrix (ECM)
HBV-SMCs were cultured in either 96-wells plates (8000 cells/well, Falcon, BD Biosciences, Billerica, MA) for quantitative immunofluorescence (QIF) analysis or in 6-well plates (100,000-200,000 cells/well, Nunc, Thermo Fisher Scientific) for Western blot analysis, all plates coated with 50 µg/ml fibronectin (Sigma-Aldrich). Cells were grown until near-confluence and treated with 15 µM $A\beta_{1-42}$ or MilliQ water for 20 hours in serum-free medium (total volume 100µl/well in 96-wells plates, 1 ml/well in 6-wells plate). To isolate ECM, cells were removed with 50 mM NH4OH-0.05% Triton X-100 (Sigma-Aldrich) and 50mM NH4OH, both incubated for 5 minutes at RT. Wells were subsequently washed with TBS pH 7.4. The remaining ECM was incubated for at least one hour with 10U/ml rq1 RNase free DNase-1 (Promega) in a Tris-sodium buffer (4.84 g/L TRIS, 0.58 g/L NaCl, 0.57 g/L MgCl2, 1.95 g/L CaCl2, pH 7.9) to remove DNA remnants and washed with TBS. Presence of tTG in the ECM was analysed using Western blot analysis. As ApoE and TG cross-links could not be detected in the ECM with Western blot analysis, the more sensitive QIF assay was used.

Quantitative immunofluorescence (QIF)
After removal of the cells in 96-wells plates, ECM was incubated overnight at 4°C with antibodies goat anti-ApoE (Q16, dilution 1:500, Santa Cruz, Dallas, TX, USA) or mouse anti-81D4 (TG cross-links, dilution 1:1000, Covalab) in Odyssey blocking buffer (Li-cor Biosciences, Lincoln, Nebraska USA) diluted 1:1 in TBS with 0.1% Tween 20 (Licor-TBST). ApoE was then detected by incubation with secondary antibody donkey anti-goat coupled to IRDye 800 (dilution 1:10,000, Li-cor Biosciences) for 1 hour at RT. TG cross-links were detected by secondary antibody donkey anti-mouse IgM coupled to biotin (Jackson Immunoresearch Laboratories Inc.), followed by incubation with Streptavidin coupled to IRDye 800 (dilution 1:8000, Li-cor Biosciences). Wells were washed extensively with TBS-T or TBS alone in between incubation steps. Presence of proteins was visualised with the Odyssey Sa Infrared imaging system (Li-cor Biosciences). Immunofluorescence was quantified using the Odyssey software by measuring the staining intensity per condition corrected for wells in which the primary antibody was omitted. Control conditions (no Aβ treatment) were set at 100% and treatment conditions were related to the control condition.

Western blot analysis
tTG protein levels in ECM were detected with Western blot analysis. For this, ECM was collected by scraping in RIPA buffer (137 mM NaCl, 20 mM Tris, 1 mM EDTA, 1% NP40, 1% sodium deoxycholate, 0.1% SDS pH 7.4) with 5 µg/ml of protease inhibitors (all Sigma-Aldrich) pepstatin A (P5318), aprotinin (A1153) and leupeptin (L2884) and 17µg/ml phenylmethylsulfonyl fluoride (PMSF, P7626). Samples were stored at -20°C until further use. Samples were mixed with Laemmli SDS sample buffer with 50mM DTT (Sigma-Aldrich) heated and subjected to 6% SDS-poly acrylamide gel electroforesis (PAGE) by loading equal volumes of samples. After gel electrophoresis, samples were transferred to a 0.2µm nitrocellulose membrane (Li-Cor Biosciences) and blocked with Licor-TBS for 1 hour at RT. Blots were incubated overnight at 4°C with primary antibody mouse anti tTG-Ab3 (1:1000, Thermo Scientific) or mouse anti-actin (1:10,000, AC-15, Abcam) in Licor-TBS with 0.1% Tween-20 (Sigma-Aldrich; Licor-TBST). Subsequently blots were incubated with secondary antibody donkey anti-mouse (dilution 1:10,000, Li-cor Biosciences), coupled to IRDye 680 (dilution 1:10,000, Li-cor Biosciences). In between incubation steps, blots were extensively washed with TBS with 0.1% Tween-20 (TBS-T) or TBS alone. Blots were visualised with the Odyssey Sa infrared imaging system (Li-Cor Biosciences). Band densities were measured with the Odyssey SA infrared imaging system. Control conditions (no Aβ treatment) were set at 100% and treatment conditions were related to the control condition.

Visualisation of cells and ECM
To visualise HBV-SMCs and remaining ECM after cell removal, pictures were taken using an Olympus CK2 microscope with Olympus DP10 camera (Olympus, Tokyo, Japan). In addition, the ECM was also stained and visualised with an antibody against collagen IV, an important component of vessel wall ECM [44]. For this, cells grown until near-confluence in 6-wells plates (100,000-200,000 cells/well) were removed as described above. The remaining ECM was blocked with 5% BSA in TBS with 0.1% TritonX-100 (TBS-T) for 1 hour at RT and incubated overnight at 4°C with a rabbit anti-collagen IV antibody (dilution 1:3000, ab6586, Abcam) in blocking buffer. Subsequently ECM was incubated with secondary antibody donkey anti-rabbit coupled to Alexa488 (dilution 1:400, Invitrogen) in blocking buffer for 1 hour at RT. ECM was washed in between incubation steps with TBS-T. Collagen IV staining was visualised with an Olympus CKX41 fluorescence microscope (Olympus) with U-CMAD3 camera (Olympus).

Viability assay
Cell viability assay was performed as described previously (Wilhelmus et al., 2007; Wilhelmus et al., 2006a). HBV-SMCs were plated in eight-well chamber slides (5600-6500 cells/well, Nunc, Thermo Fisher Scientific) and grown until near-confluence. Cells were then washed twice with serum-free medium and incubated in serum-free medium for at least

four hours. ApoE (1 μM, ApoE3L) was pre-aggregated for 30 minutes at RT in serum-free medium with 0.65 μM tTG (Zedira) and the reaction was stopped with 40 μM of the tTG activity inhibitor Z-DON [40, 41]. To block tTG activity prior to incubation with ApoE, tTG was incubated with 40 μM Z006 for 30 minutes at RT. Subsequently, cells were pre-treated for 30 minutes with 1 μM ApoE alone, pre-aggregated ApoE, or 0.65 μM tTG with 40 μM Z-DON. Incubation was continued with the addition of 20 μM $A\beta_{1-42}$ for 5 days in total volume of 120 μl. The Aβ solvent MilliQ water was used as a control. Z-DON was added to the conditions where tTG was present to prevent tTG-catalysed cross-linking of Aβ [18, 28]. Cell viability was quantified using a fluorescent Live/Dead®Viability/Cytotoxicity Kit according to the manufacturer's description (Molecular Probes, Eugene, OR, USA). The experiment was repeated three times with duplicate conditions. In four microscopic fields per well with a representative cell population live and dead cells were counted using an Olympus CKX41 fluorescence microscope at a 10X zoom (Olympus). The percentage of dead cells was calculated per well, averaged per condition.

Statistical analysis

Graphpad Prism 5 statistical software package and SPSS Statistics 20.0 were used to present and statistically analyse data. A t-test was performed to test for statistical differences between the monomers in the ApoE or ApoE/tTG condition and between the multimers in either condition. For QIF and WB analysis, one sample t-test was performed to test statistically significant difference between treatment conditions and control conditions. For viability assay analysis, group differences were statistically analysed with a one-way ANOVA using Bonferroni post-hoc testing. P-values ≤0.05 are regarded as statistically significant. All data are presented as mean±SEM.

Results

tTG binds different ApoE isoforms

In order to investigate protein-protein interaction between tTG and ApoE, we determined the relative binding affinity of tTG for different ApoE isoforms and lipidation state using Surface Plasmon Resonance (SPR) measurements. We demonstrated strong binding between tTG and all ApoE isoforms and lipidated ApoE, yielding a high association and a low dissociation of tTG for the ApoE variants in the nanomolar range (Figure 1). The SPR measurements demonstrated no apparent differences in relative binding affinity (KD) of tTG for the ApoE isoforms, i.e. ApoE2, ApoE3 and ApoE4, as well as the lipidated state (ApoE3L) (Figure 1, table). As we observed a similar relative binding affinity between the ApoE isoforms and lipidation state, we continued our experiments using the most common ApoE isoform ApoE3 [46], and the most biologically relevant and abundant form in the brain, which is lipidated ApoE3L [12].

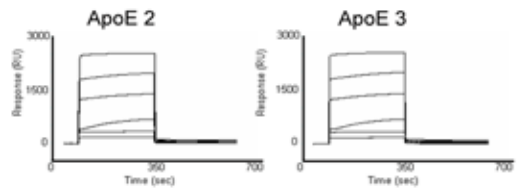

	ApoE2	ApoE3	ApoE4	ApoE3L
Relative K_D (M)	4.9×10^{-8}	3.2×10^{-8}	3.5×10^{-8}	6.77×10^{-8}

Figure 1 Protein-protein interaction between ApoE and tTG. Binding affinity of tTG for different ApoE isoforms and lipidated ApoE were analysed using SPR. Interaction of tTG with insect ApoE2, ApoE3, ApoE4 and human plasma purified ApoE3 (ApoE3L) was analysed by coating the different ApoE forms on the sensor chip and incubation with 6 different concentrations (0.32-2.6 μM) of tTG. All three different ApoE isoforms and ApoE3L demonstrated a high association with tTG on the sensor chip and a low dissociation, measured by RU over time (sec). Relative binding affinity (KD) of tTG for ApoE2, ApoE3, ApoE4 and ApoE3L was all in the nanomolar range (table). Abbreviations: ApoE = apolipoprotein E; RU = resonance units; SPR = surface plasmon resonance; tTG = tissue transglutaminase.

ApoE is a substrate for tTG-catalysed cross-linking and induces ApoE multimers

Catalytic activity of tTG induces molecular cross-links between proteins resulting in both heat- and SDS-stable protein complexes [47]. To examine whether ApoE not only binds to tTG, but is also a substrate for tTG-catalysed cross-linking, we first incubated ApoE with tTG and analysed multimerisation of ApoE (Figure 2A). Western blot analysis demonstrated that incubation of ApoE alone showed ApoE monomers and possibly ApoE dimers and trimers (Figure 2A). Co-incubation of ApoE with catalytically active tTG resulted in both a significant reduction of ApoE monomers and a significant induction of heat- and SDS-stable high molecular ApoE multimers (Figure 2A, B). In addition, co-incubation of ApoE with tTG resulted in a molecular weight reduction of the ApoE dimer and trimer (Figure 2A), in comparison to ApoE alone, suggesting a tTG-induced conformational change that increases gel mobility of these ApoE species. To study whether ApoE is a substrate for tTG-catalysed cross-linking, we co-incubated ApoE and tTG with the TG substrate 5-(biotinamido) pentylamine (BAP) and analysed tTG-catalysed incorporation of BAP into ApoE. Incorporation of BAP into both ApoE monomer as well as ApoE multimers demonstrated that ApoE is a substrate for tTG-catalysed cross-linking (Figure 2C).

To gain more insight into the characteristic of the tTG-catalysed ApoE multimers, we first analysed the formation of a β-pleated sheet structure, as ApoE, especially ApoE4 is known to obtain this conformation upon multimerisation [48]. However, we observed no incorporation of Thioflavin T in time in both incubation of ApoE alone or in combination with catalytically active tTG (Figure 2D), in contrast to the positive control $A\beta_{1\text{-}42}$ [37]. In addition, we analysed the structure of tTG-catalysed ApoE multimers using electron microscopy. We found that co-incubation of ApoE with catalytically active tTG induced an increase in large protein complexes, which in higher power magnification appeared as protein aggregates (Figure 2E). The formation of these large protein structures of ApoE was not observed upon co-incubation of ApoE and catalytically inactive tTG, by co-incubation with the calcium chelator EDTA (Figure 2E).

Active tTG colocalises with ApoE in cerebral amyloid angiopathy

In CAA, colocalisation of ApoE with the deposited Aβ has been described [8, 9]. Recently, our group found evidence that tTG is also associated with CAA [20, 21]. To investigate the relevance of tTG-catalysed cross-linking of ApoE in CAA, we stained for the presence of both ApoE and active tTG in CAA of AD post-mortem brain tissue. In control brain, anti-ApoE antibody immunoreactivity demonstrated only a weak staining of blood vessel walls of the white matter (not shown), whereas in CAA strong anti-ApoE antibody immunoreactivity colocalised with the deposited Aβ (Figure 3A-C). To determine in situ tTG activity, we incubated brain sections with the tTG specific substrate T26 and analysed possible colocalisation of Aβ and T26 in both control and CAA cases. In vessels of control cases (Figure 3D-F) and unaffected vessels in AD cases (not shown), we found light T26 staining throughout the vessel wall. In CAA in AD cases however, we observed strong T26 staining colocalising with Aβ deposition (Figure 3G-I). To determine whether the observed incorporation of T26 was explicit of tTG, we co-incubated T26 with the irreversible specific tTG inhibitor Z-DON and observed strong reduction of the T26 incorporation in CAA (Figure 3J-L). Finally, we demonstrated colocalisation of in situ active tTG with ApoE in CAA as we observed colocalisation of anti-ApoE antibody immunoreactivity with the T26 staining in CAA (Figure 3M-O).

Aβ upregulates ApoE, tTG and TG cross-links in the extracellular matrix (ECM)

As ApoE's protective effect towards Aβ-induced toxicity is suggested to act in the extracellular environment [13], we investigated Aβ-mediated effects on ApoE, tTG and TG cross-link levels in the ECM of cultured HBV-SMCs using quantitative immunofluorescence (QIF) or Western blot analysis. ECM produced by cultured HBV-SMCs was isolated and analysed as described in the materials and methods. We confirmed the complete removal of cells by visualisation of HBV-SMC-produced ECM under the microscope with transmitting light (Figure 4A, ii). In addition, we demonstrated the presence of endogenously produced ECM by HBV-SMCs using an anti-collagen IV antibody (Figure 4A, iii)

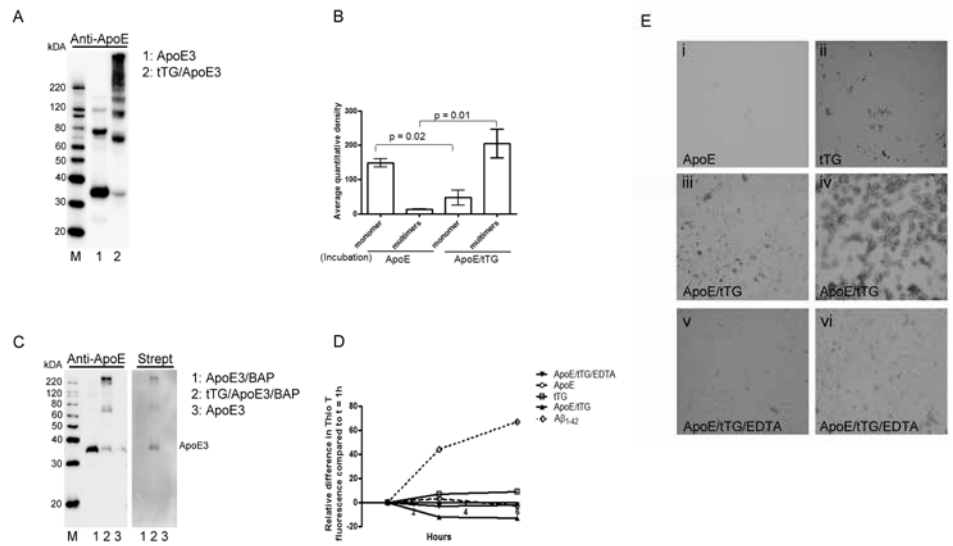

Figure 2 tTG-catalysed cross-linking induces ApoE multimers. Human plasma purified ApoE (5.3 μM) and catalytically active human tTG (5 μM) were incubated together and analysed with Western blotting (WB) as described in the materials and methods. Co-incubation of ApoE with tTG significantly reduced the levels of ApoE monomers and induced the formation of ApoE multimers (A, B). ApoE (2.6 μM) co-incubated with or without active tTG (2.5 μM), and in the presence of BAP (1 mM) was analysed using WB (C). In the presence of tTG, BAP was incorporated into both the ApoE (34 kDa) monomer and ApoE multimers (C). The formation of β-pleated sheets was tested using Thioflavin T (Thio T). $A\beta_{1\text{-}42}$ (5 μM) was used as a positive control, ApoE (5 μM), ApoE co-incubated with tTG (5 μM), tTG alone and ApoE co-incubated with tTG and EDTA, to prevent catalytic activity of tTG, was analysed. Samples were incubated at room temperature (RT) for 1, 3 and 6 hours. No β-pleated sheets were formed in either condition, except for $_{A\beta1\text{-}42}$ alone (D). The morphology of protein samples of tTG (5 μM), ApoE (5.3 μM), ApoE co-incubated with tTG, and ApoE co-incubated with tTG and EDTA (5 mM) for 6 hours at RT was analysed using electron miscroscopy (E). Co-incubation of ApoE with tTG resulted in the formation of spherical protein structures characteristic of multimers (E iii, iv (magnification of iii)) which was prevented by co-incubation with EDTA (E v and vi (magnification of v)). Zoom i-iii, v: 1850X, iv, vi: 7400X. Abbreviations: ApoE = apolipoprotein; BAP = 5-(biotinamido) pentylamine; EDTA = ethylenediaminetetraacetic acid; M = molecular weight marker; tTG = tissue transglutaminase.

to demonstrate the presence of this important constituent of the ECM [44]. The absence of intracellular proteins in the ECM samples was confirmed by the lack of the intracellular protein actin (Figure 4A, iv). HBV-SMCs treated with $A\beta_{1-42}$ demonstrated an $A\beta_{1-42}$-induced elevation of both tTG enzyme levels (217.0±23.7% of control (mean±SEM)) and ApoE levels in the ECM (136.9±12.4% of control) (Figure 4B). Interestingly, $A\beta_{1-42}$ treatment also significantly enhanced the levels of TG-cross-linked proteins in the ECM (547.9±64.1% of control) (Figure 4B). Treatment of cells with $A\beta_{1-40}$ showed no effect (not shown). Although CAA consist primarily of $A\beta_{1-40}$ [49], $A\beta_{1-42}$ is also present in the vessel wall and is regarded as the toxic form towards cerebral SMCs [45, 50].

Cross-linked ApoE does not prevent Aβ-mediated toxicity towards human primary cerebral vascular smooth muscle cells.

Aβ-mediated toxicity towards cerebrovascular, in particular SMC, cells is a key event in CAA [3]. ApoE is known to have a concentration- and isotype-dependent protective effect towards Aβ-mediated toxicity in cerebrovascular cells [13]. Our above-described data demonstrated tTG-catalysed cross-linking of ApoE. Molecular cross-linking of proteins by TGs is known to affect their biological functions [19]. In order to test whether tTG-catalysed post-translational modification of ApoE affects the protective role of ApoE towards Aβ-mediated toxicity of HBV-SMCs, we incubated these cells with Aβ and co-treated them with either ApoE or tTG-catalysed cross-linked ApoE, and analysed cellular toxicity of Aβ (Figure 4C). Treatment with $A\beta_{1-42}$ resulted in increased cell death (36.0±1.5% cell death (mean±SEM)) compared to untreated cells (8.2±0.6%), and $A\beta_{1-42}$ co-incubated with active tTG had no significant effect compared to $A\beta_{1-42}$ treatment alone (36.0±1.3%). Treatment of HBV-SMCs with ApoE demonstrated similar percentages of cell death (7.8±0.6%) compared to untreated cells. Co-incubation of Aβ with ApoE significantly reduced Aβ-mediated cell death to control levels (10.0±1.0%). In contrast, tTG-catalysed cross-linked ApoE was unable to rescue the cells from Aβ-mediated toxicity (34.4±1.5%), whereas preincubation of tTG with Z006 prevented tTG-catalysed crosslinking of ApoE and demonstrated a viability comparable to the control situation (10.3±0.9%). To prevent catalytic activity of tTG when added to the cell culture system, samples were co-incubated with the specific irreversible tTG inhibitor Z-DON [41]. Z-DON did not affect Aβ-induced cell death, as co-incubation of Z-DON with Aβ did not alter the Aβ-induced percentage of dead cells (not shown).

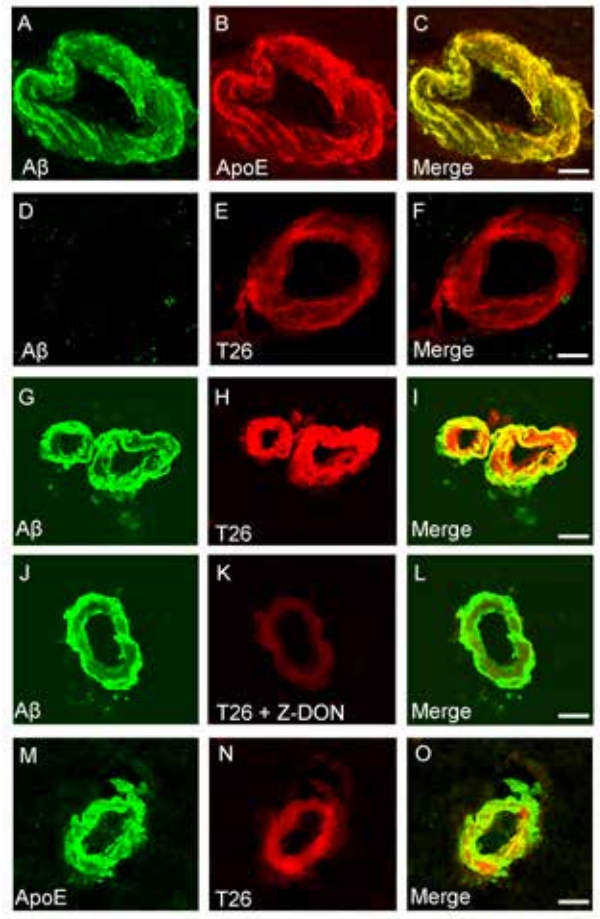

Figure 3 Colocalisation of ApoE and in situ active tTG in CAA in human post-mortem control and AD cases. Double immunofluorescence was performed with the anti-Aβ antibody and a streptavidin coupled to Alexa4594 directed against the biotin-labelled T26. Double immunofluorescence of an anti-Aβ and anti-ApoE antibody demonstrated colocalisation of Aβ and ApoE in CAA (A-C). Double immunofluorescence of an anti-Aβ and biotin-labelled T26 demonstrated presence of T26 in vessel of control cases (D-F). The anti-Aβ antibody stained CAA vessels in AD cases and colocalised with T26 staining (G-I), which was largely inhibited upon co-incubation with the irreversible tTG specific catalytic activity inhibitor Z-DON (J-L). In addition, in CAA, ApoE staining colocalised with in situ active tTG, indicated by incorporation of the tTG specific substrate T26 by endogenous tTG (M-O). Scale bar = 30μm. Abbreviations: Aβ = amyloid-beta, ApoE = apolipoprotein E, AD = Alzheimer's disease, tTG = tissue transglutaminase, CAA = cerebral amyloid angiopathy, Z-DON = Z-DON-Val-Pro-Leu-OMe.

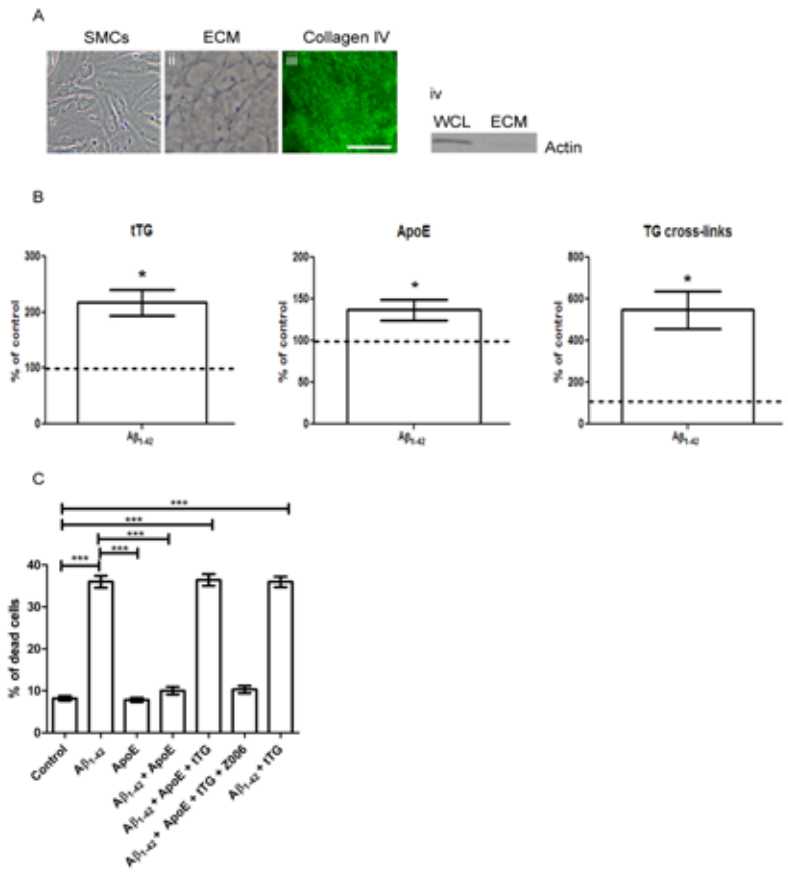

Figure 4 Effect of Aβ treatment on HBV-SMCs on ApoE, tTG and TG cross-links levels in the ECM and effect of tTG-catalysed cross-linked ApoE on Aβ-mediated toxicity towards HBV-SMCs. HBV-SMCs (A, i) and isolated ECM (A, ii) produced by HBV-SMCs were visualised with an Olympus CK2 microscope with Olympus DP10 camera with a 10X lens. ECM was stained with an anti-collagen IV antibody (A, iii) and absence of intracellular contamination was demonstrated by actin analysis of both WCL and ECM samples (A, iv). Protein levels of ApoE, tTG and TG cross-links in the ECM were determined upon treatment with $A\beta_{1\text{-}42}$ (15μM) for 20 hours and compared to control conditions. Western blot analysis showed increased tTG protein levels in ECM (217.0±23.7% of control (mean±SEM)) upon $A\beta_{1\text{-}42}$ treatment (B). $A\beta_{1\text{-}42}$ treatment also resulted in a statistically significant increase of both ApoE protein and TG cross-links in the ECM (136.9±12.4% of control, and 547.9±64.1% of control, respectively) as shown by QIF (B). Dotted lines indicate the 100% of the control condition. Graphs and blot represent the average of at least three independent experiments. Individual QIF experiments were performed in triplicate or quadruplet. Statistical analysis was performed with a one-sample t-test for WB and QIF data.

HBV-SMCs were incubated with $A\beta_{1\text{-}42}$ (20 μM), ApoE (1 μM), tTG (0.65 μM), Z006 (40 μM) or a combination of $A\beta_{1\text{-}42}$/ApoE, $A\beta_{1\text{-}42}$/tTG, $A\beta_{1\text{-}42}$/ApoE/tTG or $A\beta_{1\text{-}42}$/ApoE/tTG/Z006 for 5 days, and both dead and alive cells were analysed (C). In control cells, the percentage of dead cells was 8.2±0.6% (mean±SEM), whereas treatment with $A\beta_{1\text{-}42}$ resulted in a percentage of 36.0±1.5% of dead cells. Treatment with ApoE alone showed similar percentages of dead cells as compared to controls (7.8±0.6%). Co-incubation of tTG with $A\beta_{1\text{-}42}$ resulted in similar percentages of cell death as incubation of $A\beta_{1\text{-}42}$ alone (36.0±1.3%). Co-treatment of $A\beta_{1\text{-}42}$ with ApoE resulted in a reduction of percentage of dead cells (7.8±0.6%) comparable to untreated cells, whereas tTG-catalysed cross-linked ApoE showed no significant decrease in cell death compared to $A\beta_{1\text{-}42}$ alone (36.4±1.5%). Pretreatment of tTG with Z006 and then co-treated with $A\beta_{1\text{-}42}$ and ApoE demonstrated cell death compared to control (10.3±0.9%). Statistical analysis was performed using a one-way ANOVA (p=0.002 ANOVA) with Bonferroni post-hoc testing reaching statistically significance differences as indicated in the figure (C). The level of significance between groups or in comparison to the control is indicated as follows: ***p<0.0001. Mean±SEM are shown. Scale bar: i, ii: 50μm, iii: 80μm. Abbreviations: Aβ = amyloid-beta; ApoE = apolipoprotein, ECM = extracellular matrix, HBV-SMC = human brain vascular smooth muscle cells, QIF = quantitative immunofluorescence, tTG = tissue transglutaminase, WB = western blot, WCL = whole cell lysates.

Discussion

Aβ-induced SMC death is an important hallmark of CAA pathogenesis. Although ApoE is known to play an important role in this SMC loss in CAA, mechanisms underlying this process are unclear. In this study, we describe for the first time an interaction between tTG and ApoE and we demonstrate that ApoE is a substrate for tTG-catalysed cross-linking resulting in ApoE multimerisation. Analysis of CAA in post-mortem material of human AD cases revealed colocalisation of ApoE with in situ active tTG, hinting towards a role for tTG-ApoE interaction in CAA pathology. To gain more insight into the potential consequences of a tTG-ApoE interaction, we treated primary HBV-SMCs with Aβ and demonstrated elevated levels of tTG, ApoE and TG-catalysed cross-linking products in the ECM produced by these cells. Perhaps more important, the tTG-catalysed cross-linking of ApoE had direct consequences for ApoE's bioactivity as it was no longer able to exert its protective effect towards Aβ-mediated cerebrovascular cytotoxicity. Together, our data provide new insight into the mechanism(s) that underlie cerebrovascular degeneration in CAA.

Structural differences in ApoE affect its binding to ligands and consequently its bioactivity [10, 51, 52]. In this study, we demonstrated a strong binding affinity, i.e. in the nanomolar range, of tTG for all ApoE's tested, although we did not observe differences between ε2, ε3 and ε4 isoforms, nor for unlipidated ApoE versus lipidated ApoE. The binding site of tTG for ApoE is therefore unlikely to overlap the amino acid region responsible for the variations between ApoE isoforms, i.e. amino acid position 112 and/or 158 [12].

Previously, tTG has been demonstrated to bind and cross-link other apolipoprotein family members, i.e. ApoA-I, A-II, B and C-I [35, 36]. This suggests that binding of tTG with apolipoproteins is located within a conserved region in the apolipoprotein family. Homology between apolipoproteins is described in domains with amphipatic helices, that are suggested to play a role in phospholipid binding [53, 54], which suggest that tTG might bind in these domains of apolipoproteins. Upon binding of apolipoproteins to lipids, a conformational change occurs exposing these domains to interact with lipids [55]. Thus, tTG binding of lipidated ApoE will be hampered compared to lipid-free apolipoproteins, however lipidation did not affect the binding affinity of tTG for ApoE. Therefore, additional analyses will be necessary to determine the exact binding location of tTG to apolipoproteins. In addition to the binding site, for tTG-catalysed cross-linking to occur, glutamine and lysine residues are crucial [15]. As described-above, differences between ApoE isoforms are limited, ApoE2 (cys112, cys158), ApoE3 (cys112, arg158), and ApoE4 (arg112, arg158) [12], and do not entail glutamine and/or lysine residues [56]. Thus, ApoE isoform differences are not likely to influence glutamine and/or lysine accessibility for tTG-catalysed cross-linking, although it remains to be established which of the 30 glutamine and 12 lysine residues within the whole ApoE protein are the actual substrates for tTG's transamidation reaction [56].

Previously, apolipoprotein family members were identified as tTG substrates resulting in apolipoprotein multimers [35, 36]. Here, we demonstrated that the apolipoprotein family member ApoE is a substrate of tTG-catalysed cross-linking as well, resulting in tTG-catalysed formation of multimers of ApoE. Monomeric ApoE was strongly reduced upon incubation with catalytically active tTG, demonstrating tTG-catalysed intermolecular cross-linking between ApoE monomers into multimers. Interestingly, tTG also induced the formation of ApoE dimers and trimers with a lower kDa compared to ApoE dimers and trimers formed without the presence of tTG. This observation is in line with previous findings of our group demonstrating that tTG-catalysed cross-linking of protein and/or protein complexes induces highly stable conformational changes [17]. Similar to our findings here, tTG-catalysed cross-linking of α-synuclein monomers resulted in monomeric species that demonstrated a lower kDa compared to wild-type α-synuclein [17], probably caused by a intramolecular cross-link. Interestingly, both intra- and intermolecular tTG-catalysed cross-links are known to affect the bioactivity of these novel formed protein/protein complexes [17, 19]. Future studies are required to elucidate the biological consequences of these tTG-induced altered ApoE dimers, trimers and perhaps larger conformation altered ApoE complexes.

Spontaneous multimerisation of apolipoproteins into amyloid structure has been described [57], also for ApoE [48]. These multimers of ApoE adapted a Thioflavin T positive conformation [48] and the multimerisation of ApoE4 into Thioflavin T positive structures resulted in highly toxic aggregates leading to neuronal cell death in vitro [48]. In contrast, here we demonstrate that tTG-catalysed ApoE multimerisation did not result in Thioflavin T positive structures. This is in line with a previous report of our group on structural analysis of tTG cross-linked α-synuclein [17]. α-Synuclein and apolipoproteins both possess amphipatic helices important for lipid-binding [58], which may explain the comparable tTG-catalysed formation of Thioflavin T negative ApoE protein complexes. Together, these data suggest that tTG-catalysed protein complex formation may be of a non-amyloidogenic nature.

CAA development starts with Aβ deposition between cerebrovascular SMCs in the medial layer of the vessel wall. We previously reported the presence of increased tTG levels in the Aβ deposition in early stage CAA [21], suggesting increased production and/or secretion by SMCs. In addition, ApoE is known to be present in CAA lesions [8, 9] and Aβ-mediated cell stress of cerebrovascular cells leads to upregulation of ApoE [13]. We here demonstrated colocalisation of ApoE with in situ tTG activity in CAA suggesting tTG cross-linking activity in the affected vessel wall. In addition, we showed that extracellular levels of ApoE, tTG and TG cross-links in the ECM produced by these cells were increased. An explanation for the increased extracellular levels may be that Aβ-induced cell death results in the release of intracellular proteins into the extracellular space. However, under our experimental conditions following 20 hours of Aβ treatment, we did not observe Aβ-induced cell death (data not shown). A more likely reason therefore is translocation of tTG from inside the cell to the extracellular environment. The mechanism of tTG translocation to the extracellular environment still remains unclear, although regulation by nitric oxide [59], transport via recycling endosomes [60] and binding to fibronectin at the cell surface [61] have been suggested. However, irrespective of the mechanisms, a previous study indeed found that $A\beta_{1\text{-}42}$ treatment of neuronal cells resulted in translocation of tTG to the cell membrane [62]. Although the exact mechanism of Aβ-induced translocation needs to be elucidated, in early stages of CAA when the SMCs are still present, increased levels of Aβ in the vessel wall may lead to enhanced secretion of tTG and ApoE by SMCs into the ECM. Subsequently, tTG-catalysed cross-linking of ApoE and/or other proteins may occur. Although we indeed observed increased levels of cross-linked proteins in the ECM produced by Aβ-treated HBV-SMCs, we were unable to specifically demonstrate the presence of tTG-catalysed cross-linked ApoE in the ECM (data not shown). A likely explanation for this is the combination of low levels of ECM produced by the HBV-SMCs and the high detection limit of our assay for individual cross-linked proteins [63].

Aβ deposition in the vessel wall eventually leads to vessel wall degeneration and SMC death in both parenchymal and leptomeningeal vessels [49]. Although ApoE's exact role in the vessel wall remains elusive, in vitro studies suggest that ApoE protects cells from Aβ-induced cytotoxicity [13, 64–67]. Therefore, loss of ApoE's protective function might be involved in the cellular degeneration observed in CAA. So far, evidence pointing in this direction has been restricted to ApoE isoform and/or ApoE levels [13, 64–66]. We now provide evidence that post-translational modification of ApoE by tTG-catalysed cross-linking may offer an alternative explanation for the apparent failure of ApoE to protect against Aβ toxicity in CAA. As the protective effect of ApoE is suggested to depend on ApoE-Aβ

complex formation [64, 65, 67], cross-linked ApoE may fail to bind Aβ, resulting in impaired protection against Aβ toxicity. Future studies are required to investigate whether this tTG-driven post-translational modification of ApoE is indeed the key step in SMC loss in vivo. If so, the tTG-ApoE interaction would be an attractive therapeutic target to prevent cell death, vessel wall degeneration and consequent brain haemorrhages in CAA.

Acknowledgements

The authors thank the Netherlands Brain Bank for supplying the human brain tissue. This work was supported by a grant from The Brain Foundation of the Netherlands (number F2010(1)-06, to MMMW).

Disclosure Statement

None of the authors have any actual or potential conflicts of interest financially, or with other people or organisations that could influence this work.

References

1. Selkoe D (1991) The molecular pathology of Alzheimer's disease. Neuron 6:487–498
2. Attems J, Jellinger K, Thal DR, Van Nostrand W (2011) Review: sporadic cerebral amyloid angiopathy. Neuropathol Appl Neurobiol 37:75–93
3. Zipfel GJ, Han H, Ford AL, Lee J-M (2009) Cerebral amyloid angiopathy: progressive disruption of the neurovascular unit. Stroke 40:S16–9
4. Corder EH, Saunders AM, Strittmatter WJ, Schmechel DE, Gaskell PC, Small GW, Roses AD, Haines JL, Pericak-Vance MA (1993) Gene dose of apolipoprotein E type 4 allele and the risk of Alzheimer's disease in late onset families. Science 261:921–3
5. Saunders AM, Strittmatter WJ, Schmechel D, George-Hyslop PH, Pericak-Vance MA, Joo SH, Rosi BL, Gusella JF, Crapper-MacLachlan DR, Alberts MJ (1993) Association of apolipoprotein E allele epsilon 4 with late-onset familial and sporadic Alzheimer's disease. Neurology 43:1467–72
6. Schmechel DE, Saunders AM, Strittmatter WJ, Crain BJ, Hulette CM, Joo SH, Pericak-Vance MA, Goldgaber D, Roses AD (1993) Increased amyloid beta-peptide deposition in cerebral cortex as a consequence of apolipoprotein E genotype in late-onset Alzheimer disease. Proc Natl Acad Sci U S A 90:9649–53
7. Premkumar DR, Cohen DL, Hedera P, Friedland RP, Kalaria RN (1996) Apolipoprotein E-epsilon4 alleles in cerebral amyloid angiopathy and cerebrovascular pathology associated with Alzheimer's disease. Am J Pathol 148:2083–95
8. Namba Y, Tomonaga M, Kawasaki H, Otomo E, Ikeda K (1991) Apolipoprotein E immunoreactivity in cerebral amyloid deposits and neurofibrillary tangles in Alzheimer's disease and kuru plaque amyloid in Creutzfeldt-Jakob disease. Brain Res 541:163–6
9. Wisniewski T, Frangione B (1992) Apolipoprotein E: a pathological chaperone protein in patients with cerebral and systemic amyloid. Neurosci Lett 135:235–8
10. Strittmatter WJ, Weisgraber KH, Huang DY, Dong LM, Salvesen GS, Pericak-Vance M, Schmechel D, Saunders AM, Goldgaber D, Roses AD (1993) Binding of human apolipoprotein E to synthetic amyloid beta peptide: isoform-specific effects and implications for late-onset Alzheimer disease. Proc Natl Acad Sci U S A 90:8098–102
11. Pillot T, Goethals M, Najib J, Labeur C, Lins L, Chambaz J, Brasseur R, Vandekerckhove J, Rosseneu M (1999) Beta-amyloid peptide interacts specifically with the carboxy-terminal domain of human apolipoprotein E: relevance to Alzheimer's disease. J Neurochem 72:230–7
12. Holtzman DM, Herz J, Bu G (2012) Apolipoprotein E and apolipoprotein E receptors: normal biology and roles in Alzheimer disease. Cold Spring Harb Perspect Med 2:a006312
13. Wilhelmus MMM, Otte-Höller I, Davis J, Van Nostrand WE, de Waal RMW, Verbeek MM (2005) Apolipoprotein E genotype regulates amyloid-beta cytotoxicity. J Neurosci 25:3621–7
14. Fesus L (1993) Biochemical events in naturally occurring forms of cell death. FEBS Lett 328:1–5
15. Lorand L, Graham RM (2003) Transglutaminases: crosslinking enzymes with pleiotropic functions. Nat Rev Mol Cell Biol 4:140–56
16. Lorand L, Conrad SM (1984) Transglutaminases. Mol Cell Biochem 58:9–35
17. Segers-Nolten IMJ, Wilhelmus MMM, Veldhuis G, van Rooijen BD, Drukarch B, Subramaniam V (2008) Tissue transglutaminase modulates alpha-synuclein oligomerization. Protein Sci 17:1395–402
18. Hartley DM, Zhao C, Speier AC, Woodard G a, Li S, Li Z, Walz T (2008) Transglutaminase induces protofibril-like amyloid beta-protein assemblies that are protease-resistant and inhibit long-term potentiation. J Biol Chem 283:16790–800
19. Eitan S, Schwartz M (1993) A transglutaminase that converts interleukin-2 into a factor cytotoxic to oligodendrocytes. Science 261:106–8
20. Wilhelmus MMM, Grunberg SCS, Bol JGJM, van Dam A-M, Hoozemans JJM, Rozemuller AJM, Drukarch B (2009) Transglutaminases and transglutaminase-catalyzed cross-links colocalize with the pathological lesions in Alzheimer's disease brain. Brain Pathol 19:612–22
21. De Jager M, van der Wildt B, Schul E, Bol JGJM, van Duinen SG, Drukarch B, Wilhelmus MMM (2013) Tissue transglutaminase colocalizes with extracellular matrix proteins in cerebral amyloid angiopathy. Neurobiol Aging 34:1159–69
22. Wilhelmus MMM, van Dam A-M, Drukarch B (2008) Tissue transglutaminase: a novel pharmacological target in preventing toxic protein aggregation in neurodegenerative diseases. Eur J Pharmacol 585:464–72
23. Appelt DM, Kopen GC, Boyne LJ, Balin BJ (1996) Localization of transglutaminase in hippocampal neurons: implications for Alzheimer's disease. J Histochem Cytochem 44:1421–1427
24. Johnson GV., Cox TM, Lockhart JP, Zinnerman MD, Miller ML, Powers RE (1997) Transglutaminase activity is increased in Alzheimer's disease brain. Brain Res 751:323–329

25. Wang D-S, Uchikado H, Bennett D a, Schneider J a, Mufson EJ, Wu J, Dickson DW (2008) Cognitive performance correlates with cortical isopeptide immunoreactivity as well as Alzheimer type pathology. J Alzheimers Dis 13:53–66
26. Sárvári M, Fésüs L, Nemes Z (2002) Transglutaminase-mediated crosslinking of neural proteins in Alzheimer's disease and other primary dementias. Drug Dev Res 56:458–472
27. Dudek SM, Johnson G V (1994) Transglutaminase facilitates the formation of polymers of the beta-amyloid peptide. Brain Res 651:129–33
28. Schmid AW, Condemi E, Tuchscherer G, Chiappe D, Mutter M, Vogel H, Moniatte M, Tsybin YO (2011) Tissue transglutaminase-mediated glutamine deamidation of beta-amyloid peptide increases peptide solubility, whereas enzymatic cross-linking and peptide fragmentation may serve as molecular triggers for rapid peptide aggregation. J Biol Chem 286:12172–88
29. Ikura K, Takahata K, Sasaki R (1993) Cross-linking of a synthetic partial-length (1-28) peptide of the Alzheimer beta/A4 amyloid protein by transglutaminase. FEBS Lett 326:109–11
30. Rasmussen LK, Sørensen ES, Petersen TE, Gliemann J, Jensen PH (1994) Identification of glutamine and lysine residues in Alzheimer amyloid beta A4 peptide responsible for transglutaminase-catalysed homopolymerization and cross-linking to alpha 2M receptor. FEBS Lett 338:161–6
31. Osborne JC, Brewer HB (1977) The plasma lipoproteins. Adv Protein Chem 31:253–337
32. Law SW, Gray G, Brewer HB (1983) cDNA cloning of human apoA-I: amino acid sequence of preproapoA-I. Biochem Biophys Res Commun 112:257–64
33. Sharpe CR, Sidoli A, Shelley CS, Lucero MA, Shoulders CC, Baralle FE (1984) Human apolipoproteins AI, AII, CII and CIII. cDNA sequences and mRNA abundance. Nucleic Acids Res 12:3917–32
34. Hoeg JM, Meng MS, Ronan R, Fairwell T, Brewer HB (1986) Human apolipoprotein A-I. Post-translational modification by fatty acid acylation. J Biol Chem 261:3911–4
35. Borth W, Chang V, Bishop P, Harpel PC (1991) Lipoprotein (a) is a substrate for factor XIIIa and tissue transglutaminase. J Biol Chem 266:18149–53
36. Cocuzzi E, Piacentini M, Beninati S, Chung SI (1990) Post-translational modification of apolipoprotein B by transglutaminases. Biochem J 265:707–13
37. Wilhelmus MMM, Boelens WC, Otte-Höller I, Kamps B, de Waal RMW, Verbeek MM (2006) Small heat shock proteins inhibit amyloid-beta protein aggregation and cerebrovascular amyloid-beta protein toxicity. Brain Res 1089:67–78
38. Hyman BT, Phelps CH, Beach TG, et al (2012) National Institute on Aging-Alzheimer's Association guidelines for the neuropathologic assessment of Alzheimer's disease. Alzheimers Dement 8:1–13
39. Wilhelmus MMM, Otte-Höller I, Wesseling P, de Waal RMW, Boelens WC, Verbeek MM (2006) Specific association of small heat shock proteins with the pathological hallmarks of Alzheimer's disease brains. Neuropathol Appl Neurobiol 32:119–30
40. Schaertl S, Prime M, Wityak J, Dominguez C, Munoz-Sanjuan I, Pacifici RE, Courtney S, Scheel A, Macdonald D (2010) A profiling platform for the characterization of transglutaminase 2 (TG2) inhibitors. J Biomol Screen 15:478–87
41. Verhaar R, Jongenelen C a M, Gerard M, Baekelandt V, Van Dam A-M, Wilhelmus MMM, Drukarch B (2011) Blockade of enzyme activity inhibits tissue transglutaminase-mediated transamidation of α-synuclein in a cellular model of Parkinson's disease. Neurochem Int 58:785–793
42. Perez Alea M, Kitamura M, Martin G, Thomas V, Hitomi K, El Alaoui S (2009) Development of an isoenzyme-specific colorimetric assay for tissue transglutaminase 2 cross-linking activity. Anal Biochem 389:150–6
43. Sugimura Y, Hosono M, Wada F, Yoshimura T, Maki M, Hitomi K (2006) Screening for the preferred substrate sequence of transglutaminase using a phage-displayed peptide library: identification of peptide substrates for TGASE 2 and Factor XIIIA. J Biol Chem 281:17699–706
44. Yurchenco PD (2011) Basement membranes: cell scaffoldings and signaling platforms. Cold Spring Harb Perspect Biol 3:a004911–
45. Wilhelmus MMM, Otte-Höller I, van Triel JJJ, Veerhuis R, Maat-Schieman MLC, Bu G, de Waal RMW, Verbeek MM (2007) Lipoprotein receptor-related protein-1 mediates amyloid-beta-mediated cell death of cerebrovascular cells. Am J Pathol 171:1989–99
46. Wardell MR, Suckling PA, Janus ED (1982) Genetic variation in human apolipoprotein E. J Lipid Res 23:1174–82
47. Fesus L, Piacentini M (2002) Transglutaminase 2: an enigmatic enzyme with diverse functions. Trends Biochem Sci 27:534–539
48. Hatters DM, Zhong N, Rutenber E, Weisgraber KH (2006) Amino-terminal domain stability mediates apolipoprotein E aggregation into neurotoxic fibrils. J Mol Biol 361:932–44

49. Attems J (2005) Sporadic cerebral amyloid angiopathy: pathology, clinical implications, and possible pathomechanisms. Acta Neuropathol 110:345–59
50. Davis-Salinas J, Saporito-Irwin SM, Cotman CW, Van Nostrand WE (1995) Amyloid beta-protein induces its own production in cultured degenerating cerebrovascular smooth muscle cells. J Neurochem 65:931–4
51. LaDu MJ, Falduto MT, Manelli AM, Reardon CA, Getz GS, Frail DE (1994) Isoform-specific binding of apolipoprotein E to beta-amyloid. J Biol Chem 269:23403–6
52. Getz GS, Reardon CA (2009) Apoprotein E as a lipid transport and signaling protein in the blood, liver, and artery wall. J Lipid Res 50 Suppl:S156–61
53. De Loof H, Rosseneu M, Yang CY, Li WH, Gotto AM, Chan L (1987) Human apolipoprotein B: analysis of internal repeats and homology with other apolipoproteins. J Lipid Res 28:1455–65
54. Segrest JP, Feldmann RJ (1977) Amphipathic helixes and plasma lipoproteins: a computer study. Biopolymers 16:2053–65
55. Saito H, Lund-Katz S, Phillips MC (2004) Contributions of domain structure and lipid interaction to the functionality of exchangeable human apolipoproteins. Prog Lipid Res 43:350–80
56. Rall SC, Weisgraber KH, Mahley RW (1982) Human apolipoprotein E. The complete amino acid sequence. J Biol Chem 257:4171–8
57. Hatters DM, Howlett GJ (2002) The structural basis for amyloid formation by plasma apolipoproteins: a review. Eur Biophys J 31:2–8
58. Bussell R, Eliezer D (2003) A structural and functional role for 11-mer repeats in alpha-synuclein and other exchangeable lipid binding proteins. J Mol Biol 329:763–78
59. Santhanam L, Berkowitz DE, Belkin AM (2011) Nitric oxide regulates non-classical secretion of tissue transglutaminase. Commun Integr Biol 4:584–6
60. Zemskov E a, Mikhailenko I, Hsia R-C, Zaritskaya L, Belkin AM (2011) Unconventional secretion of tissue transglutaminase involves phospholipid-dependent delivery into recycling endosomes. PLoS One 6:e19414
61. Gaudry CA, Verderio E, Aeschlimann D, Cox A, Smith C, Griffin M (1999) Cell surface localization of tissue transglutaminase is dependent on a fibronectin-binding site in its N-terminal beta-sandwich domain. J Biol Chem 274:30707–14
62. Wakshlag JJ, Antonyak M a, Boehm JE, Boehm K, Cerione R a (2006) Effects of tissue transglutaminase on beta -amyloid1-42-induced apoptosis. Protein J 25:83–94
63. Schmid AW, Chiappe D, Pignat V, Grimminger V, Hang I, Moniatte M, Lashuel HA (2009) Dissecting the mechanisms of tissue transglutaminase-induced cross-linking of alpha-synuclein: implications for the pathogenesis of Parkinson disease. J Biol Chem 284:13128–42
64. Jordan J, Galindo MF, Miller RJ, Reardon CA, Getz GS, LaDu MJ (1998) Isoform-Specific Effect of Apolipoprotein E on Cell Survival and beta -Amyloid-Induced Toxicity in Rat Hippocampal Pyramidal Neuronal Cultures. J Neurosci 18:195–204
65. Drouet B, Fifre A, Pinçon-Raymond M, Vandekerckhove J, Rosseneu M, Guéant JL, Chambaz J, Pillot T (2001) ApoE protects cortical neurones against neurotoxicity induced by the non-fibrillar C-terminal domain of the amyloid-beta peptide. J Neurochem 76:117–27
66. Bruinsma IB, Wilhelmus MMM, Kox M, Veerhuis R, de Waal RMW, Verbeek MM (2010) Apolipoprotein E protects cultured pericytes and astrocytes from D-Abeta(1-40)-mediated cell death. Brain Res 1315:169–80
67. Whitson JS, Mims MP, Strittmatter WJ, Yamaki T, Morrisett JD, Appel SH (1994) Attenuation of the neurotoxic effect of A beta amyloid peptide by apolipoprotein E. Biochem Biophys Res Commun 199:163–70